



Analysis of Optical, Electronic and Spectroscopic Properties of (Biopolymer-SiC) Nanocomposites for Electronics Applications



Hind Ahmed¹, Ahmed Hashim^{1*} and Hayder M. Abduljalil²

¹University of Babylon, College of Education for Pure Sciences, Department of Physics, Iraq.

²University of Babylon, College of Science, Department of Physics, Iraq.

IN THIS paper, studying the effect of increase the number of SiC nanoparticles atoms on the optimized geometrical parameters, electronic and spectroscopic properties of polyvinyl alcohol. The studied structures are (PVA)(43Atom), (PVA-SiC)(35 Atom) and (PVA-SiC)(51Atom) nanocomposites. The optimization parameters included both bonds and angles. The electronic and structural properties included the (energy gap, cohesive energy, ionization potential, electron affinity, chemical hardness, chemical softness, electronegativity, electrophilicity and density of states) as well as spectral properties, which included IR and UV-Visible. This study uses Gaussian 0.9 program with help of Gaussian View 0.5 using density function theory (DFT) with local spin density approximation *B3LYP* level and *6-31G* basis sets. The results showed that the number of atoms has a direct impact on all the properties of the molecules studied. The increase of number of atoms is caused changes in spectral of (PVA) which include shift in some bonds and change in the intensities. These changes attributed to interactions of nanoparticles (SiC) with (PVA). Also, from Ultra Violet and Visible spectrum observed that absorption increases by increasing the number of atoms, this is due to the excitations of donor level electrons to the conduction band at these energies. The energy gap of the nanocomposites reduces from 6.8568 eV for (PVA) to 5.0715 eV for (PVA-SiC)(35Atom) and 4.5330 eV for (PVA-SiC)(51Atom). The total energies decreases with the increase the number of atoms forming the nanocomposites. The results showed that the nanocomposites can be used for different applications such as: solar cells, diodes, transistors, sensors, electronics gates, electronics devices.

Keywords: SiC, Gaussian, Nanocomposites, Spectral properties, FTIR, DFT.

Introduction

Nanotechnology is a field of applied sciences and technology that deals with different materials in the nanoscales ranges have large surface areas[1]. It is the application of technology and science to manipulate the matter at atomic and molecular scales[2]. Polymer nanocomposites materials have polymeric matrix reinforced with nanofillers such as nanotubes, nanosheets, nanoparticles and nanofibers etc. The physical properties of these nanocomposites mainly depend on the interaction between polymeric molecules and nanofillers [3].

Today, the studies on polymer nanocomposites have attracted much attention due to their modern different applications in the polymer nanotechnology field [4]. Poly(vinyl alcohol) is soluble polymer in water that has involved exacting interest due to its biocompatibility and hydrophilicity properties. Poly(vinyl alcohol) (PVA) is harmless and has excellent thermal stability, creation it a hopeful candidate to be used in biotechnology and biomedicine fields [5,6]. PVA present an excellent host material due to its good film morphology, combined with high flexibility. However, these properties are highly susceptible

*Corresponding author e-mail: ahmed_taay@yahoo.com

Received 11/1/2019; Accepted 19/3/2019

DOI: 10.21608/EJCHEM.2019.7154.1590

©2019 National Information and Documentation Center (NIDOC)

on humidity which reduces the durability and stability of such polymer; PVA has been mainly used as a dielectric material, membrane, or adhesive because of its high solubility in water[7]. Polyvinyl alcohol (PVA) is one type of hydrophilic polymer. It's can be mixed with other materials to get a better composite according to its usefulness[8]. Carbides of transition metals form an interesting class of materials in which anions and cations are held together by a mixture of strong ionic, covalent, and metallic bonds[9]. Different transition metal carbides showed good chemical stability and good mechanical properties with high resistance against corrosion [10] The metal lattice expands and the metal-metal distance increases upon carbide formation, the increase in metal-metal distance causes contraction of the metal d-band and therefore would give a greater density of states (DOS) near the Fermi level[11].

The DOS governs many physical properties and consequently plays an important role in solid state physics, it is important to be able to predict how the DOS will behave for different molecular structures geometries. The region of polymer nanocomposites around the nanofillers called interphase, the interphase can have less or more dense structure compared to polymer matrix depending on the interaction between polymer molecules and nanofillers (Fig. 1)[3].

The wavelength of light required for electronic transitions is typically in the UV and visible region of the electromagnetic radiation spectrum, electronic absorption spectroscopy is often called UV visible or UV-Vis spectroscopy. It is named electronic absorption spectroscopy because the absorption in the UV-visible regions involves typically electronic transitions[12]. Infrared

spectroscopy is a very useful spectroscopy tool for determining the presence of functional groups and bonding sequences in a compound by the absorption of light in the IR region of the electromagnetic spectrum[13]. DFT has proven hugely successful in the calculation of structural properties of condensed matter systems and the electronic properties of simple metals[14].

Understanding the complex interaction between polymeric material (PVA) and SiC nanoparticles, we have been made using theoretical method density functional theory (DFT). DFT is the principal method for the quantum mechanical imitation of periodic systems. it has been putative by quantum chemists and is nowadays very widely used for the imitation of energy surfaces in molecules[15]. In this paper, the effect of (SiC) nanoparticles atoms number on structural, electronic and optical properties of PVA has been studied. The (SiC) nanoparticles have good electrical, optical, thermal, chemical and mechanical properties, so it has been used in this paper as additive to PVA to use it for different electronic and optoelectronic applications.

Theoretical Part

The total energy for a system is the sum of total kinetic and potential energy, at the optimized structure that the total energy of the molecule must be at the lowest value because the molecule is at the equilibrium point this means that the resultant of the effective forces is zero. Cohesive energy is defined as the energy required to separating the condensed material into isolated free atoms. The cohesive energy is then the difference between energy per atom of the bulk material at equilibrium and the energy of a free atom in its ground state. The cohesive energy E_{coh} is given by[16]:

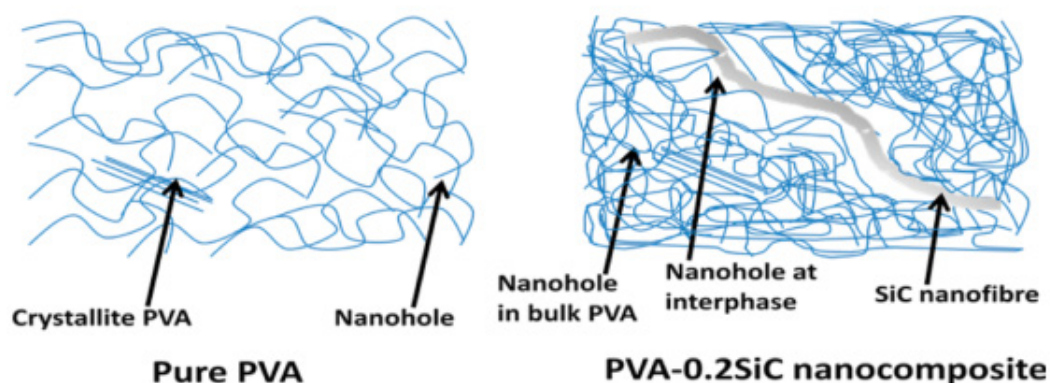


Fig. 1. (A) Free volume nanoholes in pure PVA, (B) PVA-SiC nanocomposite structure having two layers [3].

$$E_{\text{coh}} = (E_{\text{tot}} / n) - E_{\text{free}} - E_0 \dots \quad (1)$$

Where E_{tot} is the total energy. E_{free} is the free atoms, n is the number of atoms, E_0 is the vibration energy of ground states (zero-point).

The HOMO (is the molecular orbital of highest energy that is occupied by electrons) and LUMO (is the molecular orbital of lowest energy that is not occupied by electrons) are important in determining such properties as molecular reactivity and the ability of a molecule to absorb light [17]. The band gap refers to energy difference between the highest occupied molecular orbital and lowest unoccupied molecular orbital according to the Koopmans theorem [19]:

$$E_g = E_{\text{LUMO}} - E_{\text{HOMO}} \dots \quad (2)$$

energy gap not only determines the way the molecule interacts with other species, but their energy gap (frontier orbital gap) helps characterize the chemical reactivity and kinetic stability of the molecule. The ionization potential (IP) for a molecule is the amount of energy required to remove an electron from an isolated atom or molecule and expressed as the energy difference between the positive charged energy $E_{(+)}$ and the neutral $E_{(n)}$ according to the following relation:

$$\text{IP} = E_{(+)} - E_n \dots \quad (3)$$

The electron affinity (EA) of a molecule or atom is the energy change when an electron added to the neutral atom to form a negative ion and expressed as the energy difference between the neutral energy $E(n)$ and the negative charged energy $E(-)$ according to the following relation:

$$\text{EA} = E(n) - E_- \dots \quad (4)$$

In molecular orbital (MO) theory within the limitation of Koopman theorem [19], the orbital energies of the frontier orbitals are given by:

$$\text{IP} = -E_{\text{HOMO}} \dots \quad (5) \quad \text{EA} = -E_{\text{LUMO}} \dots \quad (6)$$

Where E_{HOMO} HOMO is the energy of highest occupied molecular orbital, and E_{LUMO} LUMO is the energy of lowest unoccupied molecular orbital.

The chemical hardness (η) is a measure of the resistance to charge transfer.

The theoretical definition of chemical hardness has been provided by the density functional theory as the second derivative of electronic energy with respect to the number of electrons N , for a

constant external potential $V(r)$ [20]:

$$\eta = \frac{1}{2} \frac{\partial^2 E}{\partial N^2} = \frac{1}{2} \frac{\partial \mu}{\partial N} = -\frac{1}{2} \frac{\partial^2 X}{\partial N^2} \dots \quad (7)$$

Finite difference approximation to chemical hardness gives:

$$\eta = \text{IP} - \text{EA} \dots \quad (8)$$

The global chemical softness, S , is a property of molecules that measures the extent of chemical reactivity. It is the inverse of the chemical hardness [21]:

$$S = \frac{1}{2} \frac{\partial \eta}{\partial N} = \frac{\partial N}{\partial \mu} \dots \quad (9)$$

The fundamental variation principle in density functional theory is the electronic chemical potential, where the reactivity indicator is related to how the electronic energy E of a molecule changes with changing the number of electrons N and the external potential. Parr et al. showed that for every collection of nuclei and electrons system there was electronic chemical potential K , defined as [22]:

$$K = \frac{\partial E}{\partial N} \dots \quad (10)$$

Where v is the potential due to nuclei.

Then we might define the electronegativity (It is defined as "the power of an atom in a molecule to attract electrons to itself by Pauling) as the negative of the electronic chemical potential [23]:

$$X = -K = -\frac{\partial E}{\partial N} \dots \quad (11)$$

R. Mulliken defined electronegativity as the average of the ionization energy and electron affinity as follows [24]:

$$X = \frac{(\text{IP} + \text{EA})}{2} \dots \quad (12)$$

According to Koopmans' theorem, it can be defined as the negative value for average of the energy levels of the HOMO and LUMO [17,25]:

$$X = -\frac{E_{\text{HOMO}} + E_{\text{LUMO}}}{2} \dots \quad (13)$$

Stabilization in energy when the system acquires an additional electronic charge from the environment [18]. On the other word, it can be defined as a measure of energy lowering due to maximal electron flow between donor and acceptor [20].

$$\omega = \kappa^2 \eta \dots \quad (14)$$

Where κ chemical potential is associated with the negative of the electronegativity.

Experimental Part

Silicon Carbide (SiC), it was obtained as powder from US Research Nanomaterials, Inc, USA with size (<80nm,cubic) and high purity (99%). Polyvinyl alcohol (PVA) used as powder with high purity (99.8%). The polyvinyl alcohol-Silicon Carbide nanocomposites prepared by using by casting method with concentrations (98.5 wt.%) of polyvinyl alcohol, and the Silicon Carbide (SiC) nanoparticles were added to (PVA) with changed weight percentages are (x= 0, 1.5, 3, 4.5 and 6) Wt.%. This addition was applied theoretically by using one of the famous programs in computational chemistry is *Gaussian 09(G09)* Program and Gaussian view 5.0.8 program and using density functional theory (DFT) at *B3LYP* level with *6-31G* basis set.

Results and Discussion

Figures 2-4 show the optimized structures of nanocomposites in the gas state, were obtained with the DFT method using the three-parameter hybrid-functional of Becke *B3LYP* with *6-31G* basis sets. More than one model of nanocomposites with different length of polymer chains has been tested and thus a difference in the number of atoms that forming the nanocomposites, thereby; it has

been investigation that it is possible increasing the concentration of the nanocomposites both theoretically and practically.

Table 1 shows the geometric parameters of (PVA) and (PVA-SiC)nanocomposites involved the bond length in Angstrom and bond angle in degree by using the Gaussian 09 package of programs by employing the DFT with the *B3LYP/6-31G*level. It has been deduced that the DFT method is an efficient to estimate the optimized structure of the studied molecule, that due to the DFT method characterized by its accuracy to estimate the molecular properties for any compound. The calculated values of bonds in present work are in a good agreement with theoretical study [14,26,27].

The SiC nanoparticles are caused changes in spectral of (PVA)which include shift in some bonds and change in the intensities. These changes attributed to interactions of nanoparticles with (PVA).The FTIR studies show that there is no interactions between(PVA)and(SiC)nanoparticles. Figure 5 and Table 2 show the theoretical results of FTIR obtained using the Gaussian view 5.0 program and density functional theory (DFT) with (6-31G) basis sets.

Ultra Violet and Visible spectrum is

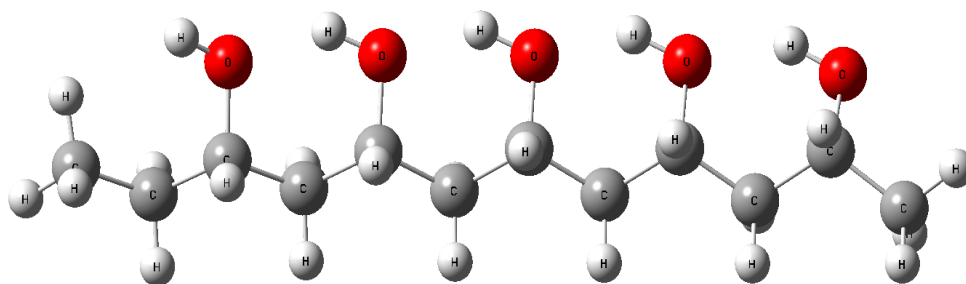


Fig. 2. Optimized geometry for (PVA) contain (43 Atom) at the *B3LYP/ 6-31G* basis set.

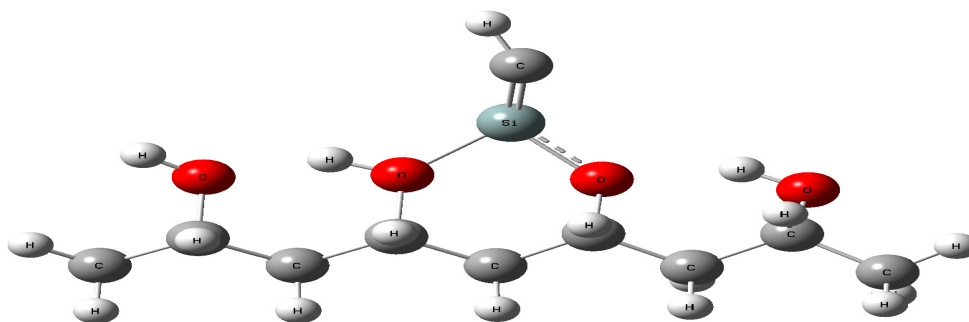


Fig. 3. Optimized geometry for (PVA-SiC) contain (35 Atom) at the *B3LYP/ 6-31G* basis set.

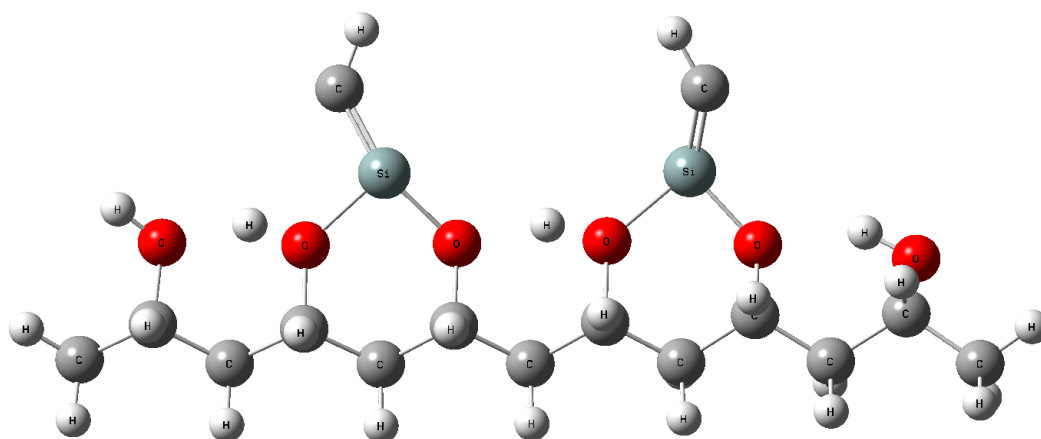


Fig. 4. Optimized geometry for (PVA-SiC) contain(51 Atom) at the B3LYP/ 6-31G basis set.

TABLE 1. Average bond lengths in (Å) and angles in degree.

Values	The optimization parameters	Linear
1.541627	(C-C)	
1.48018	(C-O)	
1.098264	(C-H)	Bonds
0.99314	(O-H)	A0
1.7546	(C:::Si)	
112.8785	(C-C- C)	Angles
109.1321	(C-O-H)	deg.

TABLE 2. The values of energy gap in (eV) of the studied structures

PVA 43 Atom			PVA-SiC 35 Atom			PVA-SiC 51 Atom		
E_{HOMO} (eV)	E_{LUMO} (eV)	E_{g} (eV)	E_{HOMO} (eV)	E_{LUMO} (eV)	E_{g} (eV)	E_{HOMO} (eV)	E_{LUMO} (eV)	E_{g} (eV)
-5.9339	0.9229	6.8568	-4.4498	0.6217	5.0715	-4.1828	0.3502	4.5330

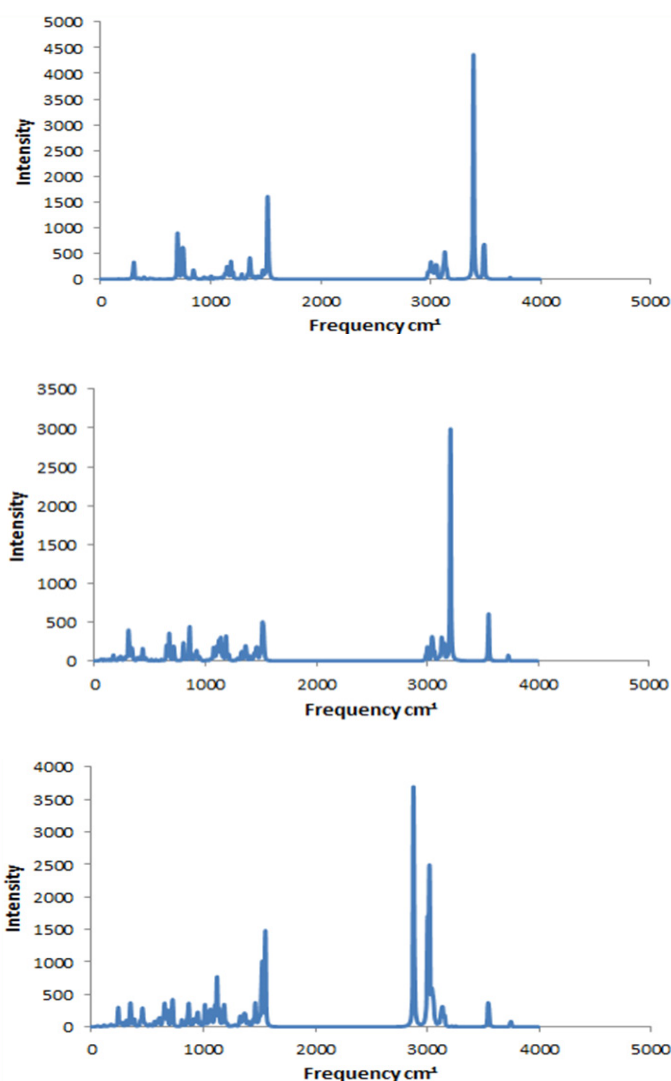


Fig. 5. IR spectrum of A-(PVA) (43 Atom), B-(PVA-SiC)(35Atom), C-(PVA-SiC)(51Atom)

dependent upon the electronic structure of the molecule. Figure 6 shows the UV-Vis spectra that theoretically obtained by using Gaussian 09 program and Gaussian view 5.0.8 program and using density functional theory (DFT) at *B3LYP* level with *6-31G* basis sets. From the figure we note that the spectrum within the limits Ultraviolet-Visible (UV-Vis) of the spectrum, because the spectrum is practically as a function of concentration, that is, the spectrum is calculated for each concentration, while theoretically the rate is taken to concentrations. Which, will calculate the highest concentration where the sample will be completely opaque only seen in the visible area of the spectrum and at a lower concentration which will be in the area of the spectrum. From Fig.

(6-c) observed that (PVA-SiC)(51 Atom) have higher UV-Vis spectra in comparison with (PVA) (43 Atom) and (PVA-SiC)(35Atom). As a result, it shows that absorption increases by increasing the number of atoms, this is due to the excitations of donor level electrons to the conduction band at these energies. The high absorbance of samples for nanocomposites at UV-Vis region attributed to the energy of photon enough to interact with atoms; the electron excites from a lower to higher energy level by absorbing a photon of known energy [28-36]. This behavior consistent with the results of researchers [37].

The energy band gap found by using equation (2). The band gap refers to energy difference

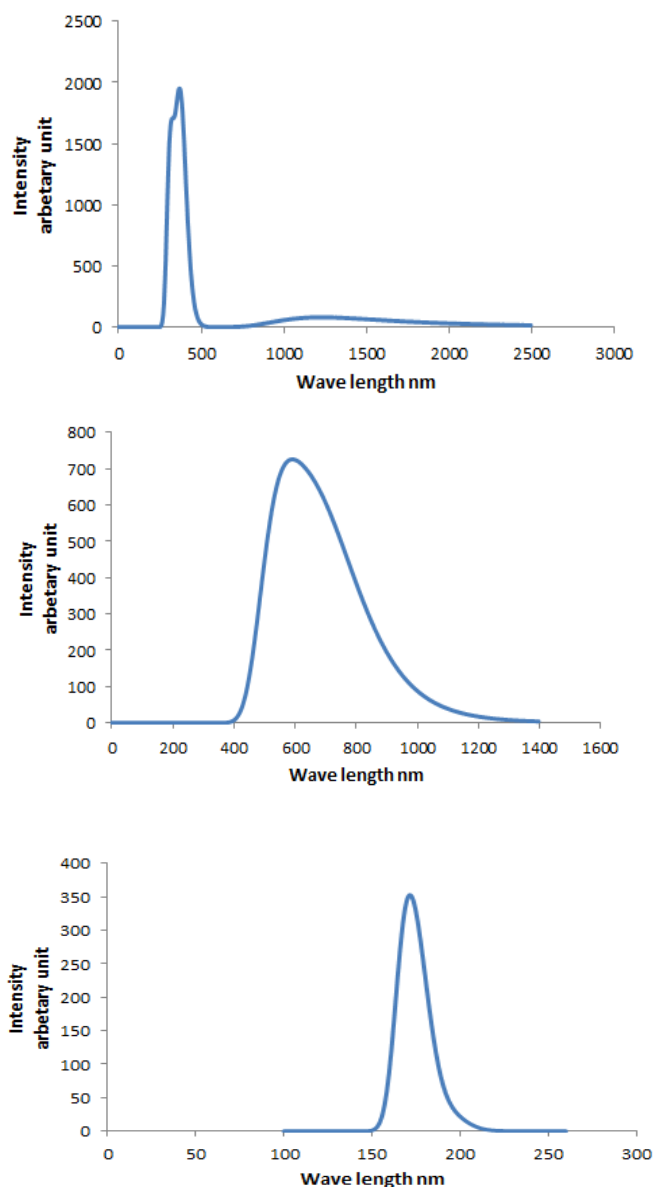


Fig. 6. UV-Vis spectrum for A- (PVA) (43 Atom), B- (PVA-SiC) (35 Atom), C- (PVA-SiC) (51 Atom) using B3LYP/6-31G

between the highest occupied molecular orbital and lowest unoccupied molecular orbital according to the Koopmans theorem. Table 2 shows the energy gap for (PVA)(43Atom), (PVA-SiC)(35Atom) and (PVA-SiC)(51Atom). Figure 7 illustrates the 3-D distribution of HOMO^s and LUMO^s for the studied nanocomposites. From this figure, the form of the nanocomposites has the same effect on both HOMO and LUMO distribution. The change of the form of the nanocomposites leads to change the map of HOMO and LUMO

distribution according to the linear combination of atomic orbitals-molecular orbital LCAOs-MO.

The addition of (SiC) nanoparticles to (PVA) led to a reduction of the energy gap from 6.8568 eV for (PVA) to 5.0715 eV and 4.5330 eV for (PVA-SiC)(35Atom) and (PVA-SiC)(51Atom) respectively. From the results of the energy gap calculated decreases with increasing the number of atoms theoretically.

The computed total energy E_T and cohesive

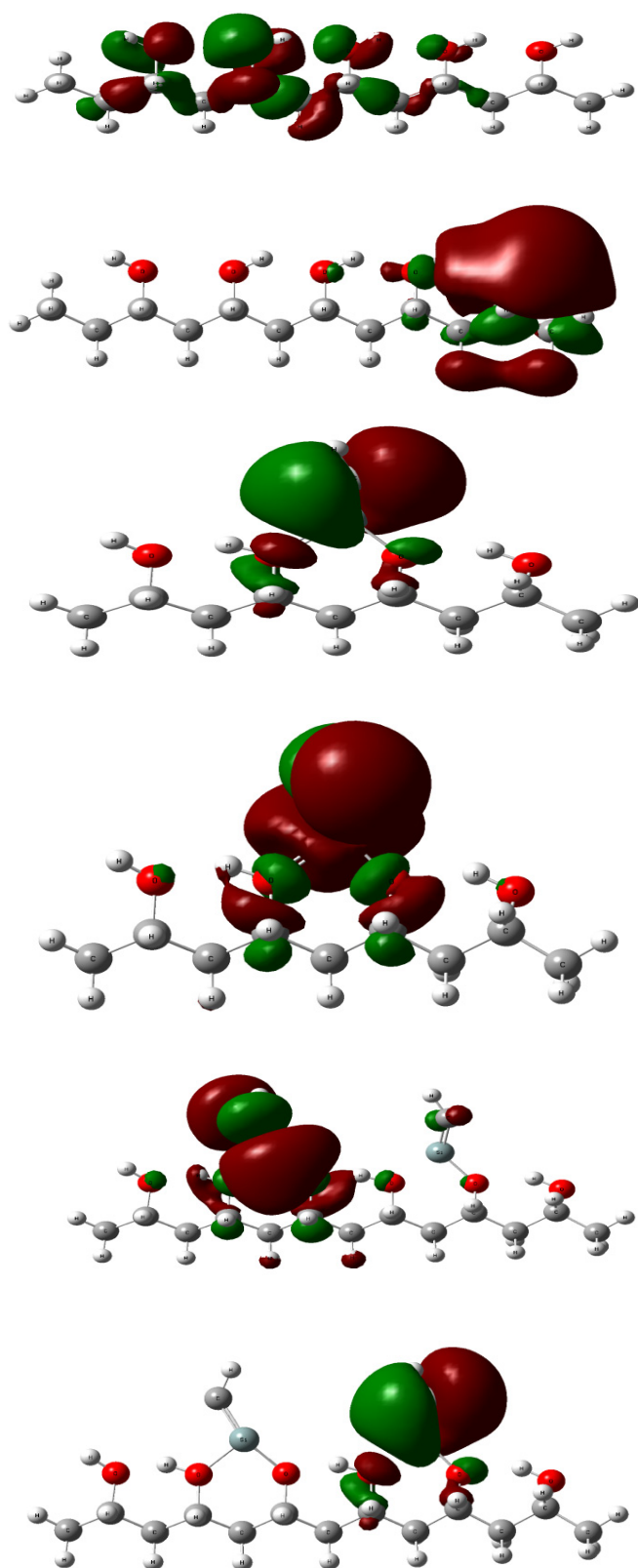


Fig. 7. The distribution of HOMO (left) and LUMO (right) for A-(PVA)(43 Atom), B-(PVA-SiC)(35 Atom), C-(PVA-SiC)(51 Atom).

energy E_{coh} [relaxation energy, E_{rlx} , defined as the difference of the total energies of the film with truncated bulk and fully relaxed structures[38-43] data shown in Table 3 suggest that it decreases (in magnitude) significantly with increase in the number of atoms for studied. The relaxation energy, E_{rlx} , does not increase with the number of layers. This indicates that the main contribution to the relaxation energy comes from the surface and sub-surface layers[38]. It is well known that the frontier molecular orbitals, the highest occupied molecular orbital HOMO and the lowest unoccupied molecular orbital LUMO, play a significant role for the reactant molecules in chemical reactions, it can be concluded that less negative E_{coh} value for nanocomposites might be related to its higher LUMO energy level. An interesting conclusion that can be drawn from these investigations is that this factor can affect the values of cohesive energies. Here, the system with larger E_{coh} is more stable. The hard molecule has a large energy gap and the soft molecule has a small energy gap. In quantum theory, changes in the electron density of system result from the mixing of suitable excited state wave functions with the ground state wave function. A small energy gap means small excitation energies to the manifold of excited states. Therefore, soft molecules with small energy gaps. Their electron density change more easily than a hard molecule, and due to that,

soft molecules will be more reactive than hard molecules.

Figure 8 illustrates the electrostatic potential ESP distribution surface of nanocomposites calculated from the total self-consistent field SCF. The ESP distributions for the nanocomposites in results from the strength of repulsion or attraction of the areas that surrounding each nanocomposite. In general, the ESP surfaces of the (PVA),(PVA-SiC) (35Atom) and (PVA-SiC) (51Atom) nanocomposites are dragged toward the positions of negative charges in each molecule means the oxygen atoms of high electronegativity[3.5 eV].

The strength of interactions can be further studied by analyzing orbital interactions between the atoms of nanocomposite, in terms of density of states DOS as shown in Fig. 9. DOS of the relax structures in the figures indicating that (PVA)(43Atom),(PVA-SiC)(35Atom) and (PVA-SiC) (51Atom) nanocomposites are energy gap decrease in the range **(6.8568eV)**, **(5.0715eV)** and **(4.5330eV)** respectively. With these values of the energy gap, we move from the insulating material to the semiconductor material. The high density of states at specific energy levels refers to that there are many states in the structure available for occupation. If there is no states can be occupied at that energy level that refers to zero density of states.

TABLE 3. The values of some electronic properties in eV of the studied structures.

Property	PVA Atoms 43	PVA-SiC Atoms 35	PVA-SiC Atoms 51
(eV) Total energy	-23101.3339	-18984.9133	28495.9986-
(eV) cohesive energy	-0.6885	-5.2744	-15.5167
(Ionization potential (eV	5.9339	4.4498	4.1828
(eV) Electron affinity	0.9229-	0.6217-	0.3502-
(eV) Electronegativity	5055,9	1.9140	1.9163
(Chemical hardness (eV	3.4284	2.5357	2.2665
(Chemical softness(eV	0.1458	0.1971	0.2206
(eV) Chemical potential	2.5055-	1.9140-	1.9163-
(Electrophilicity (eV	0.9155	0,7223	0.8101

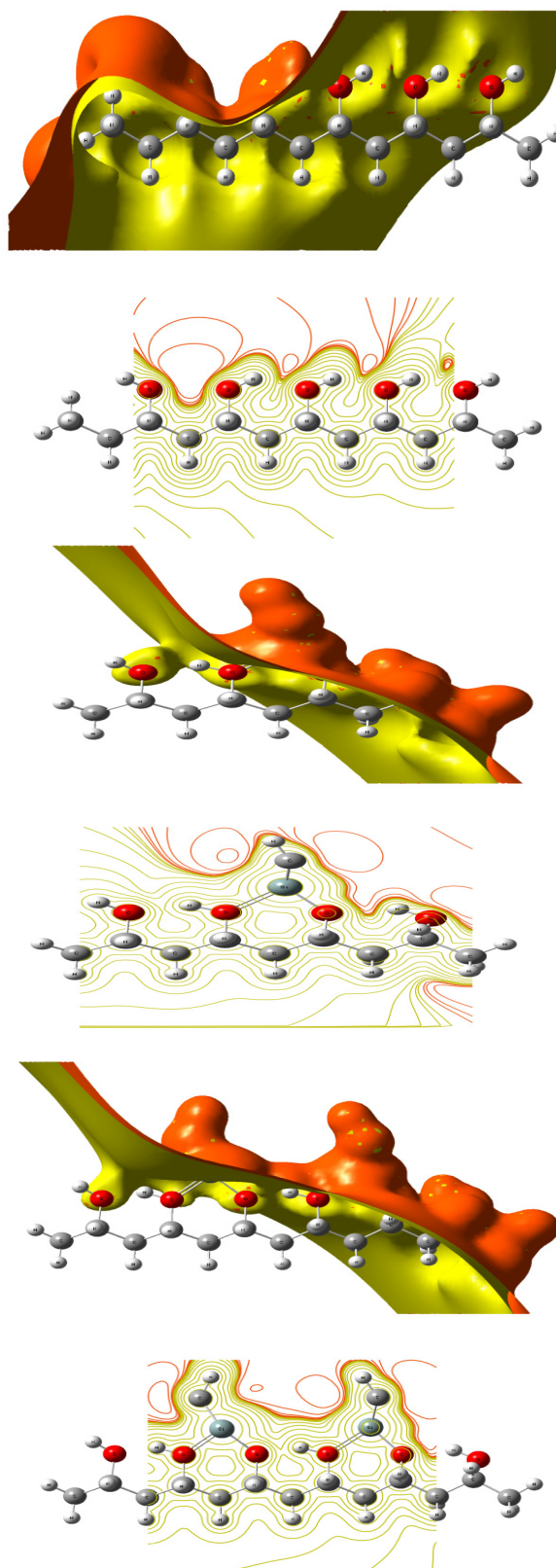


Fig. 8. The electrostatic potential distribution surface for A-(PVA)(43Atom),B-(PVA-SiC)(35 Atom),C-(PVA-SiC) (51Atom).

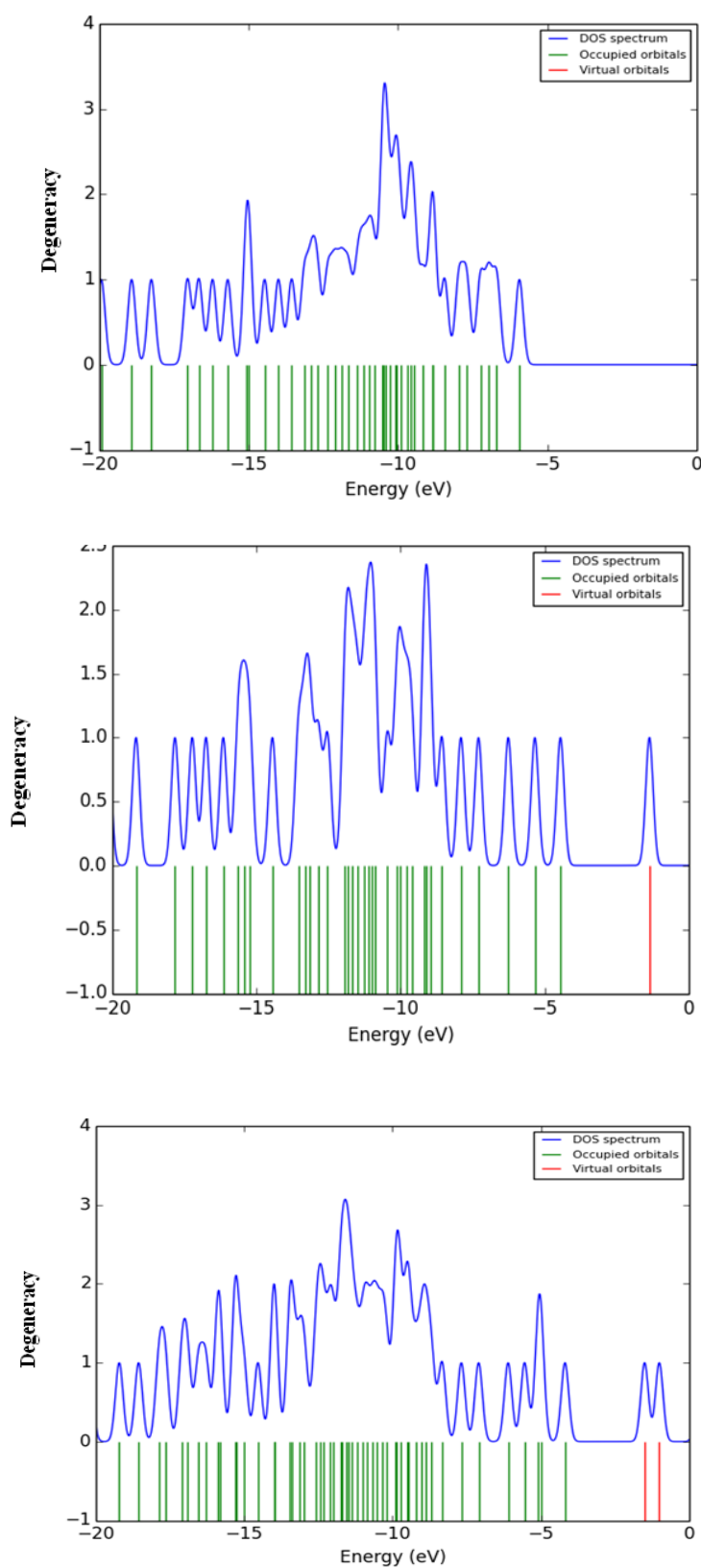


Fig. 9. Density of states as a function of bond length for a-(PVA)(43 Atom), b-(PVA-SiC)(35Atom), c-(PVA-SiC) (51Atom)

Conclusions

1. B3LYP level with 6-31G density functional theory has been proved its validity in studying the geometry optimization and calculating the geometrical parameters (angles and bonds length).
2. The absorbance of polyvinyl alcohol (PVA) increases with an increase in a number of atoms for SiC nanoparticles. The nanocomposites have high absorbance for UV energy and visible energies which are may be used for different electronic applications such as: solar cells, diodes, transistors, sensors..etc, with low cost and lightweight.
3. The present work exposes that the energy gap of (PVA-SiC)(51Atom)the largest structures equal to (4.5330eV).
4. The total cohesive energy (absolute value) increases as the number of atoms for SiC nanoparticles increase but the average cohesive energy decreases with respect to increase of the SiC nanoparticles.

The results of structural, electronic and optical properties of (PVA-SiC) nanocomposites showed that the (PVA-SiC) nanocomposites can be used for different electronics and optoelectronics applications such as: solar cells, diodes, transistors, sensors, electronics gates, electronics devices.

References

1. Patra, J. K., and Baek, K. H. Comparative study of proteasome inhibitory, synergistic antibacterial, synergistic anticandidal, and antioxidant activities of gold nanoparticles biosynthesized using fruit waste materials. *International Journal of Nanomedicine*, **11**, 4691 (2016).
2. Kumar, A., Kaur, K., and Sharma, S. Synthesis, characterization and antibacterial potential of silver nanoparticles by *Morusnigra* leaf extract. *Indian J Pharm Biol Res*, **1**(4), 16-24 (2013).
3. Sharma, S. K., Prakash, J., Sudarshan, K., Sen, D., Mazumder, S., and Pujari, P. K. Structure at Interphase of Poly (vinyl alcohol)-SiCNanofiber Composite and Its Impact on Mechanical Properties: Positron Annihilation and Small-Angle X-ray Scattering Studies. *Macromolecules*, **48**(16), 5706-5713 (2015).
4. Ningaraju, S., Prakash, A. G., and Ravikumar, H. *Egypt. J. Chem.* **62**, No. 9 (2019)
5. B. Studies on free volume controlled electrical properties of PVA/NiO and PVA/TiO₂ polymer nanocomposites. *Solid State Ionics*, **320**, 132-147 (2018).
6. Ferrández-Rives M., Aurora Beltrán-Osuna Á., J. Antonio Gómez-Tejedor Dand J. Luis Gómez Ribelles, Electrospun PVA/Bentonite Nanocomposites Mats for Drug Delivery, *Materials*, **10** (1448), (2017).
7. Hashim A., Agool I. R. and Kadhim K. J., Novel of (Polymer Blend-Fe₃O₄) Magnetic Nanocomposites: Preparation and Characterization For Thermal Energy Storage and Release, Gamma Ray Shielding, Antibacterial Activity and Humidity Sensors Applications, *Journal of Materials Science: Materials in Electronics*, **29** (12), 10369–10394 (2018).
8. Jang, J. H., and Han, J. I. Cylindrical relative humidity sensor based on poly-vinyl alcohol (PVA) for wearable computing devices with enhanced sensitivity. *Sensors and Actuators A: Physical*, **261**, 268-273 (2017).
9. Sirait, M., Gea, S., and Motlan, E. M. Effect of mixed nanoparticles ZnS and polyvinyl alcohol (PVA) against nanocomposite mechanical properties of PVA/ZnS. *American Journal of Physical Chemistry*, **3**(1), 5-8 (2014).
10. Balko, J., Csanádi, T., Sedlák, R., Vojtko, M., Kovalčíková, A., Koval, K. and Naughton-Duszová, A. Nanoindentation and tribology of VC, NbC and ZrC refractory carbides. *Journal of the European Ceramic Society*, **37**(14), 4371-4377 (2017).
11. Ham, D. J., and Lee, J. S. Transition metal carbides and nitrides as electrode materials for low temperature fuel cells. *Energies*, **2**(4), 873-899 (2009).
12. Oyama, S. T. Preparation and catalytic properties of transition metal carbides and nitrides. *Catalysis Today*, **15**(2), 179-200 (1992).
13. Norman, T. J., Magana, D., Wilson, T., Burns, C., Zhang, J. Z., Cao, D., and Bridges, F. Optical and surface structural properties of Mn²⁺-doped ZnSe nanoparticles. *The Journal of Physical Chemistry B*, **107**(26), 6309-6317 (2003).
14. MdGazzali, P. M., Kanimozhi, V., Priyadharsini, P., and Chandrasekaran, G. Structural and Magnetic properties of Ultrafine Magnesium Ferrite Nanoparticles. In *Advanced Materials Research* **938**, 128-133. Trans Tech Publications (2014).
15. Pham, N. K., Vu, N. H., Van Pham, V., Ta, H. K. T., Cao, T. M., Thoai, N., and Tran, V. C.

- Comprehensive resistive switching behavior of hybrid polyvinyl alcohol and TiO₂ nanotube nanocomposites identified by combining experimental and density functional theory studies. *Journal of Materials Chemistry C*, **6**(8), 1971-1979 (2018).
15. Dr. Valli. G and Jayalakshmi. A. Erythrina ariegate leaves extract assisted synthesis of titanium dioxide nanoparticles in an ecofriendly approach. *European Journal of Biomedical and Pharmaceutical Sciences*, **2**,1228-1236 (2015).
 16. Hugosson, H. W. A theoretical treatise on the Electronic Structure of designer Hard Materials *Doctoral Dissertation*, Acta Universitatis Upsaliensis (2001).
 17. Young, D. C. A Practical Guide for Applying Techniques to Real-World Problems (2001).
 18. Abdulsattar, M. A. Size effects of semi empirical large unit cell method in comparison with nanoclusters properties of diamond-structured covalent semiconductors. *Physica E: Low-dimensional Systems and Nanostructures*, **41**(9), 1679-1688 (2009).
 19. Hehre W. J., Radom L., Schleyer P. R. and Pople J. A., "Ab Initio Molecular Orbital Theory", John Wiley and Sons Inc, New York (1986).
 20. Oftadeh, M., Naseh, S., and Hamadianian, M. Electronic properties and dipole polarizability of thiophene and thiophenol derivatives via density functional theory. *Computational and Theoretical Chemistry*, **966**(1-3), 20-25 (2011).
 21. Sadasivam, K., and Kumaresan, R. Theoretical investigation on the antioxidant behavior of chrysoeriol and hispidulin flavonoid compounds—A DFT study. *Computational and Theoretical Chemistry*, **963**(1), 227-235 (2011).
 22. Sabin, J. R., Trickey, S. B., Apell, S. P., and Oddershede, J. Molecular shape, capacitance, and chemical hardness. *International Journal of Quantum Chemistry*, **77**(1), 358-366 (2000).
 23. Camargo, A. J., Honório, K. M., Mercadante, R., Molfetta, F. A., Alves, C. N., and da Silva, A. B. A study of neolignan compounds with biological activity against *Paracoccidioides brasiliensis* by using quantum chemical and chemometric methods. *Journal of the Brazilian Chemical Society*, **14**(5), 809-814 (2003).
 24. Shenghua, L., He, Y., and Yuansheng, J. Lubrication chemistry viewed from DFT-based concepts and electronic structural principles. *International Journal of Molecular Sciences*, **5**(1), 13-34 (2003).
 25. Barnes, C.E. Inorganic Chemistry (Catherine E. Housecroft and Alan G. Sharpe). *Journal of Chemical Education*, **80**, 747 (2003).
 26. Gupta, S. M., and Tripathi, M. A review of TiO₂ nanoparticles. *Chinese Science Bulletin*, **56**(16), 1639 (2011).
 27. Arab, A., Ziari, F., and Fazli, M. Electronic structure and reactivity of (TiO₂)_n (n= 1–10) nanoclusters: Global and local hardness based DFT study. *Computational Materials Science*, **117**, 90-97 (2016).
 28. Hashim A. and Hadi Q. Structural, electrical and optical properties of (biopolymer blend/ titanium carbide) nanocomposites for low cost humidity sensors. *Journal of Materials Science: Materials in Electronics*, **29**, 11598–11604 (2018).
 29. Hashim A. and Hadi Q. Synthesis of Novel (Polymer Blend-Ceramics) Nanocomposites: Structural, Optical and Electrical Properties for Humidity Sensors. *Journal of Inorganic and Organometallic Polymers and Materials*, **28** (4), 1394–1401 (2018).
 30. Ahmed Hashim and Aseel Hadi, Synthesis and Characterization of (MgO-Y2O3-CuO) Nanocomposites for Novel Humidity Sensor Application, *Sensor Letters*, **15**, doi:10.1166/sl.2017.3900 (2017).
 31. Agool I. R., Kadhim K. J., Hashim A., Fabrication of new nanocomposites: (PVA-PEG-PVP) blend-zirconium oxide nanoparticles) for humidity sensors, *International Journal of Plastics Technology*, **21**(2), (2017).
 32. Hadi A., Hashim A., Development of a new humidity sensor based on (carboxymethyl cellulose–starch) blend with copper oxide nanoparticles, *Ukrainian Journal of Physics*, **62**(12), (2017).
 33. Hashim A. and Hadi A., novel lead oxide polymer nanocomposites for nuclear radiation shielding applications, *Ukrainian Journal of Physics*, **62**, (11), (2017).
 34. Hind Ahmed, Hayder M. Abduljalil, Ahmed Hashim. Analysis of Structural, Optical and Electronic Properties of Polymeric Nanocomposites/Silicon Carbide for Humidity Sensors, *Transactions on Electrical and Electronic Materials*, <https://doi.org/10.1007/s42341-019-00100-2>. (2019).
 35. Hind Ahmed, Ahmed Hashim, Hayder Abduljalil, Analysis of Structural, Electrical and Electronic Properties of (Polymer Nanocomposites/ Silicon Carbide) For Antibacterial Application, *Egyptian Journal of Chemistry*, DOI: 10.21608/EJCHEM.2019.6241.1522 (2019),
 36. Ahmed Hashim and Zinah Sattar Hamad, Lower *Egypt. J. Chem.* **62**, No. 9 (2019)

- Cost and Higher UV-Absorption of Polyvinyl Alcohol/ Silica Nanocomposites For Potential Applications, *Egyptian Journal of Chemistry*, DOI: 10.21608/ejchem.2019.7264.1593 (2019)
37. Lin, F. Preparation and characterization of polymer TiO₂ nanocomposites via in-situ polymerization *Master's Thesis*, University of Waterloo (2006).
38. Bredow, T., Giordano, L., Cinquini, F., and Pacchioni, G. Electronic properties of rutile TiO₂ ultrathin films: Odd-even oscillations with the number of layers. *Physical Review B*, **70**(3), 035419 (2004).
39. Gerosa, M., Bottani, C. E., Caramella, L., Onida, G., Di Valentin, C., and Pacchioni, G. Electronic structure and phase stability of oxide semiconductors: Performance of dielectric-dependent hybrid functional DFT, benchmarked against G W band structure calculations and experiments. *Physical Review B*, **91**(15), 155201 (2015).
40. Gao, H., and Lian, K. A Comparative Study of Nano-SiO₂ and Nano-TiO₂ Fillers on Proton Conductivity and Dielectric Response of a Silicotungstic Acid-H₃PO₄-Poly (vinyl alcohol) Polymer Electrolyte. *ACS Applied Materials and Interfaces*, **6**(1), 464-472 (2013).
41. Pham, N. K., Vu, N. H., Van Pham, V., Ta, H. K. T., Cao, T. M., Thoai, N., and Tran, V. C. Comprehensive resistive switching behavior of hybrid polyvinyl alcohol and TiO₂ nanotube nanocomposites identified by combining experimental and density functional theory studies. *Journal of Materials Chemistry C*, **6**(8), 1971-1979 (2018).
42. Zhang, W., Han, Y., Yao, S., and Sun, H. Stability analysis and structural rules of titanium dioxide clusters (TiO₂)_n with n= 1-9. *Materials Chemistry and Physics*, **130**(1-2), 196-202 (2011).
43. Licon, R., and Rivas-Silva, J. F. Ab initio density functional study of MgO (001) surface with topological defects. *International Journal of Quantum Chemistry*, **104**(6), 919-928 (2005).

تحليل الخصائص البصرية، الإلكترونية والمطيافية للمترابكات النانوية (بوليمر حيوي) / للتنبيقات الإلكترونية (SiC)

هند احمد¹، احمد هاشم²، حيدر محمد عبد الجليل³

¹جامعة بابل، كلية التربية للعلوم الصرفة، قسم الفيزياء، العراق.

²جامعة بابل، كلية العلوم، قسم الفيزياء، العراق.

في البحث الحالي، تم دراسة تأثير زيادة عدد الذرات المضافة للمترابكات النانوية على الأمتلية الهندسية، الخصائص الإلكترونية والمطيافية للتراكيب المدروسة (PVA)(43Atom)، (PVA-SiC) (35Atom) و (PVA-SiC)(51Atom). تضمنت معاملات الأمتلية كلا من الأواصر والزوايا. أما الخصائص الإلكترونية والتركيبية شملت (فجوة الطاقة، طاقة الترابط، جهد التأين، الألفة الإلكترونية، الصلابة الكيميائية، الليونة الكيميائية، الكهروسالبية وكثافة الحالات) بالإضافة إلى الخصائص الطيفية، والتي شملت الأشعة تحت الحمراء والأشعة فوق البنفسجية المرئية. تستخدم هذه الدراسة برنامج Gaussian 0.9 بمساعدة Gaussian View 0.5 وباستخدام نظرية دالة الكثافة (DFT) مع تقريب الكثافة للبرم B3LYP ومجموعة الأساس G6-31. أظهرت النتائج أن عدد الذرات له تأثير مباشر على جميع خصائص الجزيئات المدروسة. تسبب زيادة عدد الذرات إلى تغيرات في طيف (PVA) والتي تشمل ازاحة في بعض الأواصر والتغيير في الشدة. هذه التغييرات تعزى إلى تفاعلات الجسيمات النانوية (SiC) مع (PVA). كما لوحظ من طيف فوق البنفسجي والمرئي أن الامتصاص يزداد بزيادة عدد الذرات، ويرجع ذلك إلى تهيج الإلكترونات من المستوى المانح إلى حزمة التوصيل عند هذه الطاقات. أما بالنسبة لفجوة الطاقة للمترابكات النانوية، فقد تناقصت من 6.8568 eV لـ (PVA) إلى 5.0715 eV لـ (PVA-SiC) (35Atom) و 4.5330 eV لـ (PVA-SiC) (51Atom)، ووجد أن الطاقات الكلية تتناقص مع زيادة عدد الذرات التي تشكل المترابكات النانوية. بينت النتائج أن المترابكات النانوية يمكن أن تستخدم في التطبيقات المختلفة مثل: الخلايا الشمسية، والديودات، و الترانزستورات، والمتحسسات، والبوابات الإلكترونية، والأجهزة الإلكترونية.